High-Performance Photonic Microwave Downconverter Based on a Frequency-Doubling Optoelectronic Oscillator

Dan Zhu, *Member, IEEE*, Shilong Pan, *Member, IEEE, Member, OSA*, Shuhong Cai, and De Ben

***Abstract*—Photonic microwave downconversion based on an optoelectronic oscillator (OEO) is interesting because the local oscillator signal is directly extracted from the RF signal, but some of the frequency components in the RF signal would leak to the oscillation signal due to the limited rejection ratio of the electrical bandpass filter in the OEO, which degrades the downconverted signal. In this paper, a high-performance photonic microwave downconverter based on a frequency-doubling OEO (FD-OEO) is proposed and demonstrated to avoid the direct degradation from the RF signal. A 20-GHz RF signal with 1-Gb/s data modulation is successfully downconverted by the FD-OEO. The phase noise at 10-kHz frequency offset of the extracted RF carrier by the FD-OEO is 14 dB lower than that extracted by a conventional OEO, and the receiver sensitivity of the downconverted signal has a 1.173-dB improvement. The downconverter needs only low-frequency devices, which may find application in phased-array antenna arrays, electronic warfare receivers, avionics, and wireless communication systems.**

***Index Terms*—Optoelectronic oscillator (OEO), downconversion, frequency-doubling.**

I. Introduction

A MICROWAVE downconverter to downconvert an RF signal to the baseband or intermediate frequency (IF) is essential for many microwave systems, such as phased-array antenna arrays [1], modern electronic warfare receivers [2], avionics [2], and wireless communication systems [3]. Conventional microwave systems usually employ electronic mixers to implement frequency downconversion, but the electronic mixers always have small operational bandwidth, poor isolation among the signal ports, and strong unwanted intermodulation products. To overcome these problems, a new concept to perform microwave downconversion in the optical domain is proposed [4]–[13]. Three key steps are generally required to realize the photonic microwave downconversion, i.e., converting the microwave signal into an optical microwave signal, mixing the optical microwave signal with an electrical local oscillator (LO) signal at an electro-optical modulator, and converting the optical signal back to an electrical signal at a low-speed photodetector (PD). Since the electro-optical modulator and PD have almost identical performance in a bandwidth of tens of nanometers, the photonic microwave downconverter is attractive for array signal processing, in which different signals are carried by different wavelengths and simultaneously downconverted to the baseband or IF by wavelength-division multiplexing [5], [6]. It is also interesting to incorporate the photonic microwave downconverter in radio-over-fiber systems because the signal to be downconverted is already optical and the optical-to-electrical conversion is more efficient in the low-frequency regime [7]–[11].

The previous works on photonic microwave downconverters were basically aimed to reduce the conversion loss [7]–[9], [12] or increase the dynamic range [11], [13], few attention is paid to the important role of the quality of the LO signal [6]. In fact, the performance of the photonic microwave downconverter is highly dependent on the quality of the LO signal since the noise and sidemodes around the LO would be downconverted to the baseband or IF. However, the generation of a high-frequency LO in the electrical domain usually involves multiple stages of frequency multiplications, leading to high phase noise and low spectral purity.

To generate the high-quality LO, one can rely on an optoelectronic oscillator (OEO) [14]. The OEO is an optoelectronic feedback loop consisting of an electro-optic modulator, an optical fiber delay line, a PD, an electrical amplifier (EA), and an electrical bandpass filter (EBPF) [15]–[17]. Due to the high-Q factor of the oscillation cavity provided by the optoelectronic feedback loop, the OEO can produce a high-spectral-purity signal with a phase noise as low as -140 dBc/Hz at 10-kHz offset at room temperature [15]. In addition, the operational frequency of the OEO can be as high as 75 GHz [6].

Previously, the OEO was used to simultaneously extract the RF carrier from an optical microwave signal and perform photonic microwave downconversion [6]. The principle is similar to the optical clock recovery and signal processing based on OEO in optical communication systems [18]–[20]. In the OEO-based clock recovery module, an incoming signal containing an optical clock with a frequency near the free-running oscillating

Manuscript received April 07, 2012; revised June 22, 2012; accepted July 23, 2012. Date of publication August 02, 2012; date of current version September 05, 2012. This work was supported in part by the Program for New Century Excellent Talents in University (NCET) under Grant NCET-10-0072, the National Basic Research Program of China (973 Program) under Grant 2012CB315705, the National Natural Science Foundation of China under Grant 61107063, the Ph.D. Programs Foundation of the Ministry of Education of China under Grant 20113218120018, the Open Research Program of the State Key Laboratory of Millimeter Waves under Grant K201207, Jiangsu Planned Projects for Postdoctoral Research Funds under Grant 1102054C, and the Fundamental Research Funds for the Central Universities under Grant NS2012046.

The authors are with the Microwave Photonics Research Laboratory, College of Electronic and Information Engineering, Nanjing University of Aeronautics and Astronautics, Nanjing 210016, China, and also with the State Key Laboratory of Millimeter Waves, Nanjing 210096, China (e-mail: pans@ieee.org).

Color versions of one or more of the figures in this paper are available online at http://ieeexplore.ieee.org.

Digital Object Identifier 10.1109/JLT.2012.2211096

frequency is introduced into the OEO loop, so the OEO is injection locked. The optical clock is then extracted while other components in the injected signal are suppressed [18]. With the extracted optical clock, optical signal processing, such as format conversion and signal regeneration, can be performed in the electro-optic modulator in the OEO. Compared with the optical clock recovery from a return-to-zero (RZ) or non-return-to-zero (NRZ) communication system, the carrier extraction from the optical microwave signal has a much higher requirement. For the RZ or NRZ signal, the clock always presents in the notches of the electrical spectrum since the major power of the information are located in the range from DC to 70% of the frequency of the clock [21]. In that case, even a high-Q Fabry–Perot filter is enough to effectively recover the optical clock [22]. However, for the optical microwave signal, the baseband signal is first upconverted to an RF carrier and then modulated on the optical carrier, so the major power of the information is located around the RF carrier. The closer the frequency of the component and that of the RF carrier is, the higher the power will be. As a result, it would be very hard to obtain a high-quality RF carrier using a conventional OEO since some of the frequency components in the RF signal would leak to the extracted RF carrier due to the limited rejection ratio of the EBPF.

In addition, the conventional OEO for RF carrier extraction and photonic microwave downconversion can only operate at a maximal frequency limited by the bandwidth of the electrical or electro-optical devices in the OEO loop. To extend the frequency range, frequency-doubling OEO (FD-OEO) was proposed [23], [24]. Tsuchida proposed a FD-OEO including a high-frequency EA and an electrical frequency divider [23]. Pan and Yao performed a theoretical as well as an experimental study on PolM-based FD-OEO [24], which has the capability of extracting both prescaled and line-rate clocks from a high-speed degraded optical signal using only low-frequency devices. But the application of the FD-OEO in the RF carrier extraction and photonic microwave downconversion is not reported.

In this paper, a novel photonic microwave downconverter based on an FD-OEO is proposed and demonstrated. Since the center frequency of the EBPF in the FD-OEO is half the frequency of the RF carrier, the frequency components around the carrier could not directly leak to the modulator; thus, the extracted RF carrier has a high quality, which ensures a high-performance microwave downconversion. In addition, the FD-OEO allows photonic microwave downconversion of a high-frequency signal with low-frequency device only. A theory is developed. Although the unwanted frequency components would still be downconverted to the baseband, they have a large conversion loss, so the downconverted signal will not be evidently degraded. An experiment is carried out to comparatively study the performance of the proposed photonic microwave downconverter and the downconverter based on a conventional fundamental frequency OEO (FF-OEO). Results show that the phase noise at 10-kHz offset of the 10-GHz LO signal extracted by the FD-OEO is about 14 dB lower than that extracted by the FF-OEO. The bit error rate (BER) curves of the 1-Gb/s signal downconverted by the FD-OEO and the FF-OEO are also measured, which show again that the data downconverted by the FD-OEO have better quality than that downconverted by the FF-OEO.

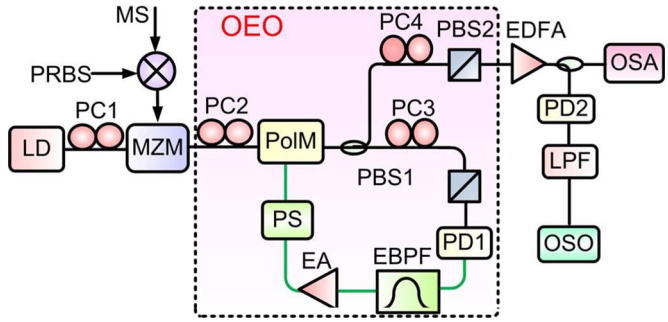

Fig. 1. Schematic diagram of the proposed photonic microwave downconverter using a PolM-based FD-OEO. (LD: laser diode; PC: polarization controller; MZM: Mach–Zehnder Modulator; PolM: polarization modulator; PBS: polarization beam splitter; MS: microwave source; EDFA: erbium-doped fiber amplifier; PD: photodetector; EA: electrical amplifier; EBPF: electrical bandpass filter; PRBS: pseudorandom bit sequence; PS: phase shifter; LPF: low-pass filter; OSA: optical spectrum analyzer; OSO: optical sampling oscilloscope.)

II. Principle

The schematic diagram of the photonic microwave downconverter based on the FD-OEO is shown in Fig. 1. A microwave source (MS) is mixed with a pseudorandom bit sequence (PRBS) data to generate an RF signal for downconvertion. A lightwave from a laser diode is modulated by an RF signal to be downconverted at a Mach–Zehnder modulator (MZM). The modulated optical signal is fiber coupled to a PolM via a polarization controller (PC, PC2). The PolM is connected to two polarization beam splitters (PBSs) via two other PCs (PC3 and PC4). The PolM in conjunction with the PCs and the polarizers is equivalent to a two-output-port intensity modulator (IM) [16], [17]. One output of the IM is fed back to the PolM via the RF port to form an OEO loop. Since an oscillator requires a positive feedback loop, PC3 is adjusted to let the output of PBS1 equivalent to linear intensity modulation [16]. A PD (PD1) is used in the OEO loop to perform optical-to-electrical conversion. To select the oscillation frequency, an EBPF is incorporated. An EA is also incorporated to ensure the loop gain higher than unity. The OEO can be a FF-OEO when PC4 is adjusted to let the output of PBS2 equivalent to intensity modulation biased at the quadrature transmission point (QTP), or a FD-OEO if PC4 is adjusted to let the output of PBS2 equivalent to intensity modulation biased at the minimum transmission point (MITP) [16].

Similar to the optical clock recovery in [16], when an optical microwave signal containing an RF carrier at a frequency of f_m is injected into the FD-OEO, an oscillation exactly at $f_m/2$ would be started in the OEO although the input optical microwave signal contains no distinct $f_m/2$ component. This is because the noise in the OEO would occasionally introduce a very small $f_m/2$ component. Once the $f_m/2$ component is present, it would be captured and amplified by the OEO. The amplified $f_m/2$ component is then fed back into the PolM-based IM and modulates the later injected signal. With the modulation, the $f_m/2$ component in the electrical modulation signal and the f_m component in the injection signal are mixed to generate a new $f_m/2$ component, which greatly enhances the existing $f_m/2$ component. This positive feedback would finally lead to

an oscillation at the frequency of $f_m/2$ and thus a high-quality RF carrier at $f_m/2$ is obtained. Once the OEO is oscillating at $f_m/2$, the optical microwave signal would multiplied with the optical intensity transfer function of the PolM-based IM in the upper branch,

$$T = \alpha\left[1 + \cos\left(\beta \sin\frac{\omega_m t}{2} + \phi_b\right)\right] \tag{1}$$

where $\omega_m = 2\pi f_m$, α is the transmission factor, β is the phase modulation index, and ϕ_b is a static phase term introduced by PC4. Let $\phi_b = 0$ via adjusting PC4, we have

$$T = \alpha\left[1 + J_0 + 2\sum_{k=1}^{\infty} J_{2k}(\beta)\cos(k\omega_m t)\right] \tag{2}$$

where J_n is the nth-order Bessel function of the first kind. From (2), we can see that the optical microwave signal is mixed with a LO frequency of f_m. If a low-pass filter (LPF) is followed, the RF signal would be downconverted to the baseband.

To theoretically study the performance of the photonic microwave downconverter based on the FD-OEO, a model for the injection-locking FD-OEO is developed. For comparison, the performance of the photonic microwave downconverter based on the FF-OEO is also investigated.

For simplicity, we assume the injected optical signal contains a DC and two sinusoidal components at ω_0 and ω_1

$$p(t) = p_0[1 + m_0\sin(\omega_0 t) + m_1\sin(\omega_1 t)] \tag{3}$$

where ω_0 and ω_1 are the angular frequencies of the RF carrier and the undesired disturbance (e.g., noise or frequency component of the data signal), p_0 is the average optical power, m_n $(n = 0, 1)$ is the modulation depth. In practice, the amplitude of the RF carrier is much greater than that of the disturbance, i.e., $m_1 \ll m_0$.

Based on [16], when the signal expressed by (3) is injected into the FF-OEO, the OEO will be injection locked if ω_0 is very close to the oscillating frequency of the free-running OEO. The disturbance frequency would also appear in the output of the OEO if it is in the passband of the EBPF. Other high order terms, such as $2\omega_0 - \omega_1$ or $2\omega_1 - \omega_0$, should also exist, but it is reasonable to ignore them since their power would be very small considering a small-signal modulation. Therefore, the steady-state oscillating signal at the RF port of the PolM should have the form

$$V(t) = V_2\sin(\omega_0 t + \phi_0) + V_3\sin(\omega_1 t + \phi_1) \tag{4}$$

where V_2, V_3 are the amplitudes and ϕ_0, ϕ_1 are the phases of the signals at ω_0 and ω_1, respectively. The transmission function of the PolM-based IM in the OEO loop is given by

$$h(t) = 1 + m_2\sin(\omega_0 t + \phi_0) + m_3\sin(\omega_1 t + \phi_1) \tag{5}$$

where $m_2 = \pi V_2/V_\pi$, $m_3 = \pi V_3/V_\pi$, V_π is the half-wave voltage of the PolM.

The injected optical signal is firstly modulated by $V(\mathrm{t})$, then converted into an electrical signal at the PD, amplified by the EA, and filtered by the EBPF, which can be then written as

$$\begin{aligned} V_1(t) = g[&(m_0 + m_2\cos\phi_0)\sin(\omega_0 t) \\ &+ m_2\sin\phi_0\cos(\omega_0 t)] \\ &+ kg[(m_1 + m_3\cos\phi_1)\sin(\omega_1 t) \\ &+ m_3\sin\phi_1\cos(\omega_1 t)] \end{aligned} \tag{6}$$

where g is the open-loop voltage gain, k is the relative voltage loss for the ω_1 component caused by the EBPF, $0 < k < 1$.

At the steady state, $V_1(t) = V(t)$, so we obtain

$$\begin{cases} V_2 = g\sqrt{[m_0 + m_2\cos\phi_0]^2 + [m_2\sin\phi_0]^2} \\ \phi_0 = \arctan\frac{m_2\sin\phi_0}{m_0 + m_2\cos\phi_0} \\ V_3 = kg\sqrt{[m_1 + m_3\cos\phi_1]^2 + [m_3\sin\phi_1]^2} \\ \phi_1 = \arctan\frac{m_3\sin\phi_1}{m_1 + m_3\cos\phi_1}. \end{cases} \tag{7}$$

Equation (7) results in (8a)–(8d), shown at the bottom of the page.

Because V_3 and V_2 are the amplitudes of voltage, V_3/V_2 should be positive for $0 < k < 1$. Considering V_3/V_2 should be equal to m_1/m_0 when $k = 1$ for small-signal modulation, the solutions to (7) are

$$\phi_0 = 0, \phi_1 = 0, V_3/V_2 = km_1/[m_0 + (1-k)m_2] \tag{9a}$$

$$\begin{aligned} \phi_0 = \pi, \phi_1 = \pi, V_3/V_2 = km_1/[m_0 + (k-1)m_2] \\ \text{if } \{(m_1 > m_3 \text{ and } m_0 > m_2) \text{ or} \\ (m_1 < m_3 \text{ and } m_0 < m_2)\}. \end{aligned} \tag{9b}$$

$$\phi_0 = 0, \phi_1 = 0, V_3/V_2 = km_1/[m_0 + (1-k)m_2] \tag{8a}$$

$$\begin{cases} \phi_0 = 0, \phi_1 = \pi, V_3/V_2 = km_1/[m_0 + (1+k)m_2] \text{ if } m_1 > m_3 \\ \phi_0 = 0, \phi_1 = \pi, V_3/V_2 = km_1/[(k-1)m_2 - m_0] \text{ if } m_1 < m_3 \end{cases} \tag{8b}$$

$$\begin{cases} \phi_0 = \pi, \phi_1 = 0, V_3/V_2 = km_1/[m_0 - (1+k)m_2] \\ \text{if } m_0 > m_2 \\ \phi_0 = \pi, \phi_1 = 0, V_3/V_2 = km_1/[(1-k)m_2 - m_0] \\ \text{if } m_0 < m_2 \end{cases} \tag{8c}$$

$$\begin{cases} \phi_0 = \pi, \phi_1 = \pi, V_3/V_2 = km_1/[m_0 + (k-1)m_2] \\ \text{if } \{(m_1 > m_3 \text{ and } m_0 > m_2) \text{ or } (m_1 < m_3 \text{ and } m_0 < m_2)\} \\ \phi_0 = \pi, \phi_1 = \pi, V_3/V_2 = km_1/[(k+1)m_2 - m_0] \\ \text{if } \{m_1 < m_3 \text{ and } m_0 > m_2) \text{ or } (m_1 > m_3 \text{ and } m_0 < m_2)\} \end{cases} \tag{8d}$$

For the photonic microwave downconverter based on the FD-OEO, according to [16], the OEO will be injection locked if $\omega_0/2$ is very close to the oscillating frequency of the free-running OEO. The disturbance frequency would be downconverted to ω_1-$\omega_0/2$. Other high order terms, such as $3\omega_0/2$-ω_1 can be reasonably ignored since their power is very small. Therefore, the steady-state oscillating signal at the RF port of the PolM can be written as

$$V(t) = V_2 \sin(0.5\omega_0 t + \phi_0) + V_3 \sin[(\omega_1 - 0.5\omega_0)t + \phi_1]. \quad (10)$$

Again, the signal is then mixed with the injected optical signal at the PolM-based IM, converted into an electrical signal at the PD, amplified by the EA, and filtered by the EBPF. After a cycle, we obtain a new expression for the signal

$$\begin{aligned} V_1(t) = {} & g[(m_2 \cos\phi_0 + 0.5m_0m_2 \sin\phi_0)\sin(0.5\omega_0 t) \\ & + (m_2 \sin\phi_0 + 0.5m_0m_2 \cos\phi_0)\cos(0.5\omega_0 t)] \\ & + kg\{(m_3 \cos\phi_1 + 0.5m_1m_2 \sin\phi_0) \\ & \times \sin[(\omega_1 - 0.5\omega_0)t + \phi_1] \\ & + (m_3 \sin\phi_1 + 0.5m_1m_2 \cos\phi_0) \\ & \times \cos[(\omega_1 - 0.5\omega_0)t + \phi_1]\}. \end{aligned} \quad (11)$$

$V_1(t)$ should be equal to $V(t)$, so we get (12), shown at the bottom of the page.

From (12), we have (13a)–(13e), shown at the bottom of the page.

Again, V_3/V_2 should be positive for $0 < k < 1$. For small-signal modulation, the solutions to (12) are

$$\begin{aligned} & \phi_0 = \pi/4, \phi_1 = \pi/4 \text{ or } \phi_0 = 5\pi/4, \phi_1 = 5\pi/4, \\ & V_3/V_2 = km_1/(2 + m_0 - 2k) \end{aligned} \quad (14a)$$

$$\begin{aligned} & \phi_0 = \pi/4, \phi_1 = 5\pi/4 \text{ or } \phi_0 = 5\pi/4,\ \phi_1 = \pi/4, \\ & V_3/V_2 = km_1/(2 + m_0 + 2k), \text{ if } m_3 < 0.5m_1m_2 \end{aligned} \quad (14b)$$

$$\begin{aligned} & \phi_0 = 3\pi/4, \phi_1 = 3\pi/4, \\ & V_3/V_2 = km_1/(2 - m_0 + 2k) \\ & \qquad \text{if } \{(m_0 < 2 \text{ and } m_3 < 0.5m_1m_2)\}. \end{aligned} \quad (14c)$$

To give a quantitative comparison of the V_3/V_2 (disturbance to signal ratio) for the FF-OEO- and FD-OEO-based downconverters, a numerical simulation based on (9) and (14) is performed. Assume $m_0 = 0.4, m_1 = 0.04$, i.e., the amplitude of the original disturbance is 10 dB lower than that of the carrier. Since the low-noise EA in the OEO always has a low saturation power, we let $m_2 = 0.3$. Fig. 2 shows the calculated V_3/V_2 as a function of k. It can be seen that the disturbance to signal ratio of the oscillation signal in the FD-OEO is generally smaller than that in the FF-OEO. In practice, we would carefully adjust the phase shifter (PS) in the OEO to achieve a lowest disturbance

$$\begin{cases} V_2 = g\sqrt{(m_2 \cos\phi_0 + 0.5m_0m_2 \sin\phi_0)^2 + (m_2 \sin\phi_0 + 0.5m_0m_2 \cos\phi_0)^2} \\ \phi_0 = \arctan\frac{m_2 \sin\phi_0 + 0.5m_0m_2 \cos\phi_0}{m_2 \cos\phi_0 + 0.5m_0m_2 \sin\phi_0} \\ V_3 = kg\sqrt{(m_3 \cos\phi_1 + 0.5m_1m_2 \sin\phi_0)^2 + (m_3 \sin\phi_1 + 0.5m_1m_2 \cos\phi_0)^2} \\ \phi_1 = \arctan\frac{m_3 \sin\phi_1 + 0.5m_1m_2 \cos\phi_0}{m_3 \cos\phi_1 + 0.5m_1m_2 \sin\phi_0} \end{cases} \quad (12)$$

$$\begin{aligned} & \phi_0 = \pi/4, \phi_1 = \pi/4 \\ & \text{or } \phi_0 = 5\pi/4, \phi_1 = 5\pi/4, V_3/V_2 = km_1/(2 + m_0 - 2k) \end{aligned} \quad (13a)$$

$$\begin{cases} \phi_0 = \pi/4, \phi_1 = 5\pi/4, V_3/V_2 = km_1/(2 + m_0 + 2k) \\ \text{if } m_3 < 0.5m_1m_2 \\ \phi_0 = \pi/4, \phi_1 = 5\pi/4, V_3/V_2 = km_1/(2k - 2 - m_0) \\ \text{if } m_3 > 0.5m_1m_2 \end{cases} \quad (13b)$$

$$\begin{cases} \phi_0 = 3\pi/4, \phi_1 = 3\pi/4, V_3/V_2 = km_1/(m_0 + 2k - 2) \\ \text{if } \{(m_0 < 2 \text{ and } m_3 > 0.5m_1m_2) \text{ or } (m_0 > 2 \text{ and } m_3 < 0.5m_1m_2)\} \\ \phi_0 = 3\pi/4, \phi_1 = 3\pi/4, V_3/V_2 = km_1/(2 - m_0 + 2k) \\ \text{if } \{(m_0 < 2 \text{ and } m_3 < 0.5m_1m_2) \text{ or } (m_0 > 2 \text{ and } m_3 > 0.5m_1m_2)\} \end{cases} \quad (13c)$$

$$\begin{cases} \phi_0 = 5\pi/4, \phi_1 = \pi/4, V_3/V_2 = km_1/(2 + m_0 + 2k) \\ (m_3 < 0.5m_1m_2) \\ \phi_0 = 5\pi/4, \phi_1 = \pi/4, V_3/V_2 = km_1/(2k - 2 - m_0) \\ (m_3 > 0.5m_1m_2) \end{cases} \quad (13d)$$

$$\begin{cases} \phi_0 = 7\pi/4, \phi_1 = 7\pi/4, V_3/V_2 = km_1/(2 - m_0 - 2k) \\ (m_0 < 2) \\ \phi_0 = 7\pi/4, \phi_1 = 7\pi/4, V_3/V_2 = km_1/(m_0 - 2 - 2k) \\ (m_0 > 2) \end{cases} \quad (13e)$$

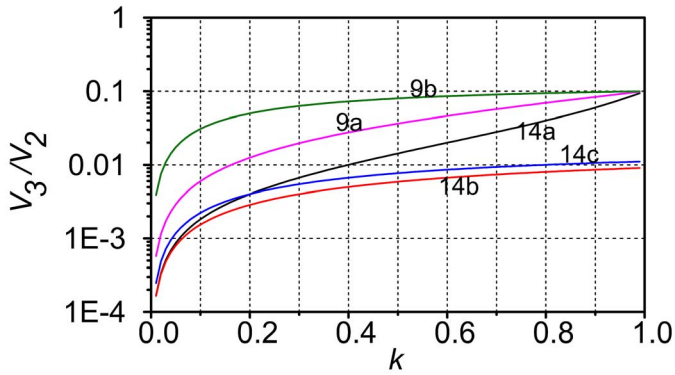

Fig. 2. Calculated disturbance to signal ratio of the oscillation signal in the FF-OEO and FD-OEO as a function of k.

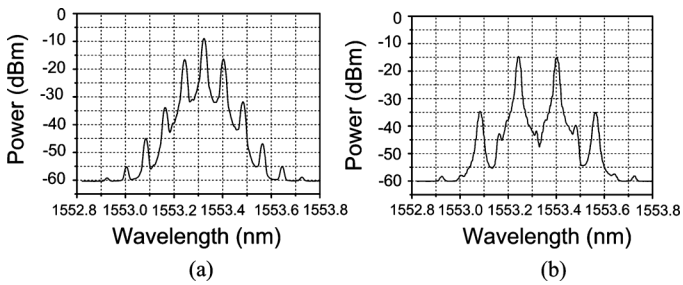

Fig. 3. Optical spectra at the output of PBS2 for (a) the PolM-based FF-OEO and (b) the PolM-based FD-OEO.

to signal ratio. In that case, the disturbance to signal ratio has about 10-dB improvement in the FD-OEO for $0.8 < k < 1$.

III. Experiment and Discussions

An experiment based on the setup shown in Fig. 1 is performed. The RF signal to be downconverted is generated by mixing a sinusoidal signal with an electrical 1-Gb/s PRBS (word length $2^{31}-1$) data signal at a mixer. The mixer has a frequency range of 6–22 GHz for the RF/LO port, and 0–1 GHz for the IF port. The sinusoidal signal is produced by an MS (Agilent E8257D), and the PRBS is generated by a pulse pattern generator (Anritsu MP1763). The RF signal with a power of 10 dBm is converted into an optical microwave signal at a 40-GHz MZM (Versawave Inc.), and then sent to the PolM-based OEO to perform downconversion.

The OEO consists of a PolM, two PBSs, two PDs, an erbium-doped fiber amplifier (EDFA), an EBPF, an EA, and a PS. The major parameters are as follows: the PolM (Versawave Inc.) has a bandwidth of 40 GHz; PD1 has a bandwidth of 10 GHz, and a responsivity of 0.88 A/W; the EBPF has a bandwidth of 11.34 MHz and a center frequency of 9.957 GHz; the gain of the EA is about 40 dB; and PD2 has a bandwidth of 40 GHz and a responsivity of 0.65 A/W. The two PBSs are connected to the PolM via two PCs to form a dual-output-port IM. One output of the IM is fed back to the RF port of the PolM to form an optoelectronic loop, and the other port serves as the output port of the downconverter. To select the downconverted signal, an electrical LPF with a bandwidth of 1.9 GHz is connected to the PD. The EDFA is used to increase the power of the optical signal to a satisfactory level.

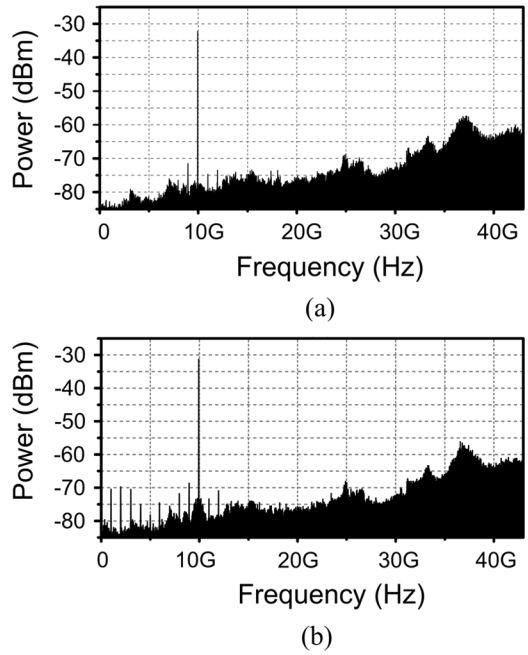

Fig. 4. Electrical spectra of the 10-GHz RF carrier extracted from 20-GHz RF signals with 1-Gb/s data modulation by (a) the FD-OEO and (b) the FF-OEO.

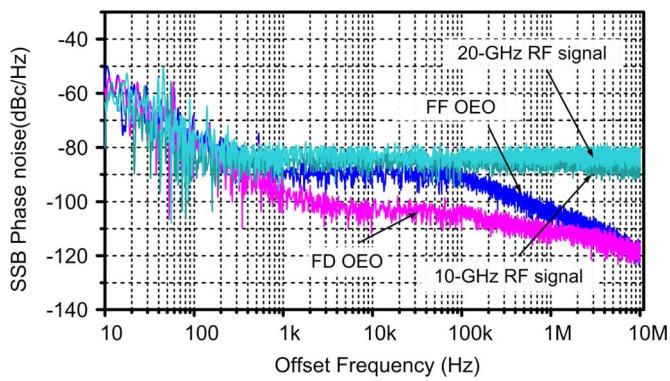

Fig. 5. Phase noise spectra of the 20-GHz, 10-GHz RF signals with 1-Gb/s data modulation and 10-GHz RF carriers extracted by the FF-OEO and the FD-OEO, respectively.

The electrical spectrum is measured by an electrical spectrum analyzer (ESA) with a build-in phase noise measurement module (Agilent E4447A, 3 Hz–43 GHz) and the optical spectrum is monitored by an optical spectrum analyzer (OSA) (Yokogawa AQ6370C) with a resolution of 0.02 nm. In addition, a 40-GHz optical sampling oscilloscope (OSO) (Agilent 86100A) is used to observe the eye diagrams.

According to [16], the PolM-based OEO can be an FF-OEO or a FD-OEO, depending on the setting of PC4. To demonstrate that the downconverter based on an FD-OEO has better performance than that based on an FF-OEO, a comparative study is performed. For the photonic microwave downconverter based on FF-OEO, PC4 in the upper branch is adjusted to let the obtained optical field be equivalent to an output of an MZM biased at the QTP, with the optical spectrum shown in Fig. 3(a), and the carrier frequency of the RF signal to be downconverted is set to be 9.957 GHz, while for the photonic microwave downconverter based on FD-OEO, PC4 in the output port is adjusted

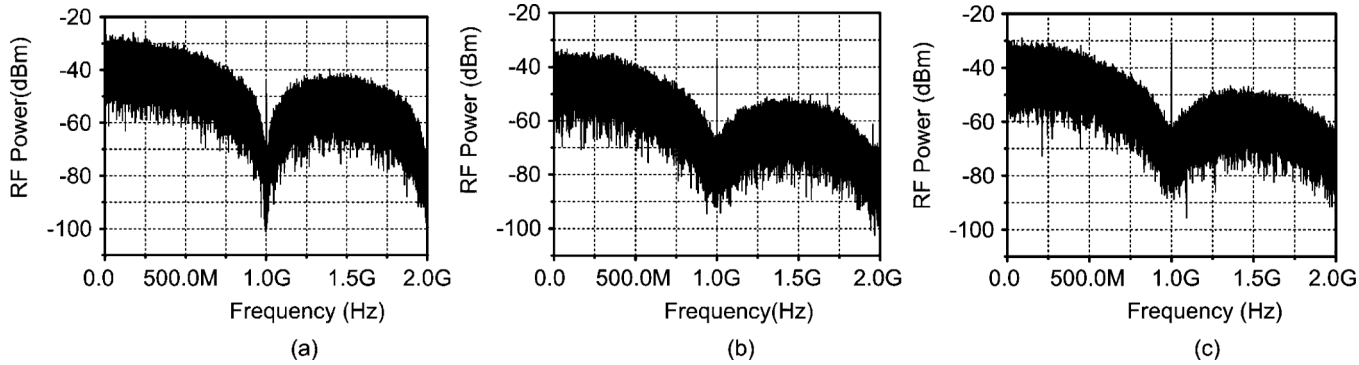

Fig. 6. Electrical spectra of (a) 1-Gb/s PRBS, and the downconverted signals by (b) the FF-OEO and (c) the FD-OEO.

to let the obtained optical field be equivalent to an output of an MZM biased at the MITP, with the optical spectrum shown in Fig. 3(b), and the carrier frequency of the RF signal to be downconverted is set to be 19.915 GHz. The modulation depth and electrical power of both signals are set to be the same. The power of the LO signal was set to be 8 dBm in our experiments.

Fig. 4 shows the electrical spectra of the oscillation signals in the OEO. The electrical spectra are taken using the ESA by introducing a coupler between EBPF and EA. As can be seen from Fig. 4(b), the data signal is evidently leaked through the EBPF to the oscillation signal of the FF-OEO, while for the FD-OEO, the spectrum is much clearer since the data signal is distributed in the 20-GHz span. In addition, some spectral components present in the low-frequency regime in Fig. 4(b). This is because the downconverted signal in the FF-OEO is also contained in the optical signal sent to PD1, which is further leaked to the oscillation signal due to the limited rejection ratio of the EBPF. This would not happen in the FD-OEO, since the downconverted signal in the OEO loop is in the 10-GHz span, which contributes positively to the optoelectronic oscillation.

Fig. 5 show the single-sideband phase noise spectra of the RF signals and the 10-GHz RF carriers extracted from the RF signals. The phase noise of the 10- and 20-GHz RF signals to be downconverted is almost the same. After the FF-OEO, the 10-GHz RF carrier is extracted, but the phase noise at the 10–100-kHz frequency offset is only $\sim$3 dB less than that of the RF signal, showing that most of the disturbance is leaked to the oscillation signal. For the 10-GHz RF carrier extracted by the FD-OEO, the phase noise at 10–100-kHz frequency offset is more than 20 dB lower than that of the data signal. Especially, the phase noise is -105.5 and -91.4 dBc/Hz at 10-kHz frequency offset for the RF carriers extracted by the FD-OEO and FF-OEO, respectively, indicating a 14-dB phase noise improvement by the FD-OEO.

With the RF carrier extracted by the OEO, photonic microwave downconversion can be performed. The electrical spectrum in Fig. 6(a) is taken after the pulse pattern generator (Anritsu MP1763) to show the spectrum of the 1-Gb/s PRBS source; and Fig. 6(b) and (c) shows the electrical spectra of the downconverted 1-Gb/s data by the FF-OEO and the FD-OEO, respectively, with the electrical spectra taken after the LPF. It can be seen that both FF-OEO and FD-OEO can perform photonic microwave downconversion. It should be noted that the FD-OEO can implement photonic microwave downconversion of 20-GHz RF signal using 10-GHz device only.

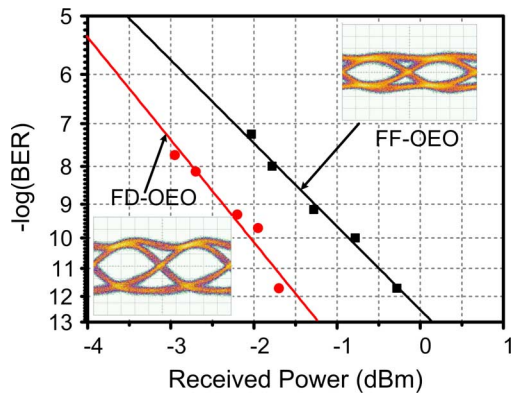

Fig. 7. BER curves of the signals downconverted by the FF-OEO and the FD-OEO.

The BER curves of the signals downconverted by the FD-OEO and FF-OEO are also measured, as shown in Fig. 7. At a BER of 10^{-10}, the FF-OEO-based photonic microwave downconverter introduces 1.173 dB more power penalty than the FD-OEO based one. The eye diagrams of the downconverted signals are also shown as the insets in Fig. 7.

These experimental results agree very well with the theoretical predictions, i.e., the proposed photonic microwave downconverter performs better than a conventional OEO based downconverter.

IV. Conclusion

A high-performance photonic microwave downconverter based on an FD-OEO was proposed. A theoretical model was developed for the comparative study of the performance between the proposed scheme and the photonic microwave downconverter based on a conventional FF-OEO. Numerical results show that the proposed scheme has much better performance. The theoretical prediction was validated by an experiment. The phase noise at 10-kHz frequency offset of the extracted RF carrier by the proposed scheme was 14 dB lower than that extracted by the conventional OEO. In addition, the receiver sensitivity of the downconverted signal by the proposed downconverter was 1.173 dB less than that downconverted by the conventional OEO.

REFERENCES

[1] K. E. Alameh, "Frequency downconverter for high-capacity fibre grating based beamformers for phased arrays," *Electron. Lett.*, vol. 35, no. 1, pp. 66–67, Jan. 1999.

[2] A. Agarwal, T. Banwell, and T. K. Woodward, "Optically filtered microwave photonic links for RF signal processing applications," *J. Lightw. Technol.*, vol. 29, no. 16, pp. 2394–2401, Aug. 2011.

[3] C.-S. Brès, S. Zlatanovic, A. O. J. Wiberg, and S. Radic, "Reconfigurable parametric channelized receiver for instantaneous spectral analysis," *Opt. Exp.*, vol. 19, no. 4, pp. 3531–3541, Feb. 2011.

[4] T. E. Darcie and B. Glance, "Optical heterodyne image-rejection mixer," *Electron. Lett.*, vol. 22, no. 15, pp. 825–826, Jul. 1986.

[5] T. Kuri, H. Toda, and K.-I. Kitayama, "Dense wavelength-division multiplexing millimeter-wave-band radio-on-fiber signal transmission with photonic downconversion," *J. Lightw. Technol.*, vol. 21, no. 6, pp. 1510–1517, Jun. 2003.

[6] W. Shieh, S. X. Yao, G. Lutes, and L. Maleki, "Microwave signal mixing by using a fiber-based optoelectronic oscillator for wavelength-division multiplexed systems," in *Opt. Fiber Commun. Conf. Tech. Dig.*, 1997, pp. 358–359.

[7] C. K. Sun, R. J. Orazi, and S. A. Pappert, "Efficient microwave frequency conversion using photonic link signal mixing," *IEEE Photon. Technol. Lett.*, vol. 8, no. 1, pp. 154–156, Jan. 1996.

[8] R. Helkey, J. C. Twichell, and C. Cox, III, "A down-conversion optical link with RF gain," *J. Lightw. Technol.*, vol. 15, no. 6, pp. 956–961, Jun. 1997.

[9] K. J. Williams and R. D. Esman, "Optically amplified downconverting link with shot-noise-limited performance," *IEEE Photon. Technol. Lett.*, vol. 8, no. 1, pp. 148–150, Jan. 1996.

[10] K.-I. Kitayana and R. A. Griffin, "Optical downconversion from millimeter-wave to IF-band over 50 km-long optical fiber link using an electroabsorption modulator," *IEEE Photon. Technol. Lett.*, vol. 11, no. 2, pp. 287–289, Feb. 1999.

[11] J. M. Fuster and J. Marti, "Optimization of the dynamic range in optically amplified harmonic downconverting fiber-optic links," *IEEE Photon. Technol. Lett.*, vol. 11, no. 7, pp. 877–879, Jul. 1999.

[12] V. R. Pagán, B. M. Haas, and T. E. Murphy, "Linearized electrooptic microwave downconversion using phase modulation and optical filtering," *Opt. Exp.*, vol. 19, no. 2, pp. 883–895, Jan. 2011.

[13] S. J. Strutz, P. Biernacki, L. Nichols, and K. J. Williams, "Demonstration of a wide-band image rejection microwave downconverter," *IEEE Photon. Technol. Lett.*, vol. 12, no. 6, pp. 687–689, Jun. 2000.

[14] X. S. Yao and L. Maleki, "Optoelectronic oscillator for photonic systems," *IEEE J. Quantum Electron.*, vol. 32, no. 7, pp. 1141–1149, Jul. 1996.

[15] X. S. Yao and L. Maleki, "Ultra-low phase noise dual-loop optoelectronic oscillator," in *Proc. Opt. Fiber Commun. Conf. Tech. Digest*, 1998, pp. 353–354.

[16] S. Pan and J. Yao, "Optical clock recovery using a polarization-modulator-based frequency-doubling optoelectronic oscillator," *J. Lightw. Technol.*, vol. 27, no. 16, pp. 3531–3539, Aug. 2009.

[17] D. Zhu, S. Pan, and D. Ben, "Tunable frequency-quadrupling dual-loop optoelectronic oscillator," *IEEE Photon. Technol. Lett.*, vol. 24, no. 3, pp. 194–196, Feb. 2012.

[18] X. S. Yao and G. Lutes, "A high-speed photonic clock and carrier recovery device," *IEEE Photon. Technol. Lett.*, vol. 8, no. 5, pp. 688–690, May 1996.

[19] L. Huo, Y. Dong, C. Lou, and Y. Gao, "Clock extraction using an optoelectronic oscillator from high-speed NRZ signal and NRZ-to-RZ format transformation," *IEEE Photon. Technol. Lett.*, vol. 15, no. 7, pp. 981–983, Jul. 2003.

[20] J. Lasri, P. Devgan, R. Tang, and P. Kumar, "Ultralow timing jitter 40-Gb/s clock recovery using a self-starting optoelectronic oscillator," *IEEE Photon. Technol. Lett.*, vol. 16, no. 1, pp. 263–265, Jan. 2004.

[21] P. J. Winzer and R. J. Essiambre, "Advanced modulation formats for high-capacity optical transport networks," *J. Lightw. Technol.*, vol. 24, no. 12, pp. 4711–4728, Dec. 2006.

[22] X. Zhou, C. Lu, P. Shum, H. H. M. Shalaby, T. H. Cheng, and P. D. Ye, "A performance analysis of an all-optical clock extraction circuit based on Fabry-Perot filter," *J. Lightw. Technol.*, vol. 19, no. 5, pp. 603–613, May 2001.

[23] H. Tsuchida, "Subharmonic optoelectronic oscillator," *IEEE Photon. Technol. Lett.*, vol. 20, no. 17, pp. 1509–1511, Sep. 2008.

[24] S. Pan and J. Yao, "Multichannel optical signal processing in NRZ systems based on a frequency-doubling optoelectronic oscillator," *IEEE J. Sel. Topics Quantum Electron.*, vol. 16, no. 5, pp. 1460–1468, Sep./Oct. 2010.

Dan Zhu (M'12) received the B.S. and Ph.D. degrees in electronics engineering from Tsinghua University, Beijing, China, in 2004 and 2009, respectively.

In July 2009, she joined the Research Department of Radar Signal Processing, No. 14 Research Institute, China Electronics Technology Group Corporation, as a Researcher. In May 2011, she joined the Photonic Microwave Research Laboratory, College of Electronic and Information Engineering, Nanjing University of Aeronautics and Astronautics, Nanjing, China. Her current research interests include terahertz wave generation and optical signal processing.

Shilong Pan (S'06–M'09) received the B.S. and Ph.D. degrees in electronics engineering from Tsinghua University, Beijing, China, in 2004 and 2008, respectively.

He joined the College of Electronic and Information Engineering, Nanjing University of Aeronautics and Astronautics, Nanjing, China, in 2010, where he is currently a Full Professor and Director of Photonic Microwave Research Laboratory. From 2008 to 2010, he was a Postdoctoral Research Fellow in the Microwave Photonics Research Laboratory, University of Ottawa, Ottawa, ON, Canada. He has authored or co-authored more than 80 papers, including over 50 papers in refereed journals and over 30 papers in conference proceeding. His current research interests include fiber amplifiers and lasers, microwave photonics, optical signal processing, and optical metrology.

Dr. Pan is a member of the Optical Society of America, the IEEE Photonics Society, and the IEEE Microwave Theory and Techniques Society.

Shuhong Cai, biography not available at the time of publication.

De Ben, biography not available at the time of publication.